Bi_2Te_3 photoconductive detectors on Si

Juanjuan Liu,[1,2] Yaoyao Li,[1] Yuxin Song,[1,a)] Yingjie Ma,[1] Qimiao Chen,[1,2] Zhongyunshen Zhu,[2,3] Pengfei Lu,[4] and Shumin Wang[1,5,b)]
[1]*State Key Laboratory of Functional Materials for Informatics, Shanghai Institute of Microsystem and Information Technology, Chinese Academy of Sciences, Shanghai 200050, China*
[2]*School of Electronic, Electrical and Communication Engineering, University of Chinese Academy of Sciences, Beijing 100049, China*
[3]*School of Physical Science and Technology, ShanghaiTech University, Shanghai 200031, China*
[4]*State Key Laboratory of Information Photonics and Optical Communications Institute of Information Photonics and Optical Communications, BUTP, Beijing 100876, China*
[5]*Department of Microtechnology and Nanoscience, Chalmers University of Technology, Gothenburg 41296, Sweden*

(Received 9 December 2016; accepted 26 March 2017; published online 5 April 2017)

The peculiar properties of the gapless surface states with a Dirac cone shaped energy dispersion in topological insulators (TIs) enable promising applications in photodetection with an ultra-broad band and polarization sensitivity. Since many TIs can be easily grown on silicon (Si) substrates, TIs on Si could make an alternative route for photon detection of Si photonics. We present good device performances of a Si-based single-crystal bismuth telluride (Bi_2Te_3) photoconductive detector. Room temperature photo responses to 1064 nm and 1550 nm light illumination were demonstrated. Linear dependences of the photocurrent on both the incident light power and the bias voltage were observed. The main device parameters including responsivity and quantum efficiency were extracted. *Published by AIP Publishing*. [http://dx.doi.org/10.1063/1.4979839]

The integrated circuit (IC) industry has rapidly developed following Moore's Law for over half a century. However, Moore's law is reaching its end when the transistors are finally scaled down to several nanometers, and the quantum effects and heat dissipation problems have become dominant.[1] Silicon (Si) photonics[2] have emerged as one of a few potential technologies to extend the lifetime of Moore's Law, or, in other words, to open the "post Moore era." Si photonics can provide high transmission speed, high bandwidth, low power consumption, low heat dissipation, etc., utilizing the advantages of light over electrons. In recent years, many significant breakthroughs of Si based passive and active building blocks on and in Si have been demonstrated including waveguides, electro-optic modulators, ultrafast photodetectors, fiber-to-waveguide couplers, and lasers.[3] Among all the elementary components, a high performance near infrared photodetector is crucial to make a high speed optical link for either optical telecommunications or interconnects.[4] Conventionally, there are two kinds of absorbent materials at the telecom wavelength utilized for photon detection on Si: germanium(Ge)-on-Si[5] and III-V-on-Si.[6] Here, we have put forward a topological insulator (TI) based photodetector on Si, which is compatible with complementary metal-oxide-semiconductor (CMOS) technology and can be monolithically integrated on Si.

TIs are an emerging class of quantum matter with bulk band-gap and spin-momentum locked gapless surface states that are protected from back scattering or localization by time-reversal symmetry.[7] Bismuth telluride (Bi_2Te_3) together with Bi_2Se_3 and Sb_2Te_3 was theoretically predicted[8] and experimentally proved[7] to be a typical 3-dimensional (3D) TI with a single Dirac cone on the surface. Molecular beam epitaxy (MBE),[9] chemical vapor deposition,[10] and pulsed laser deposition techniques[11] have been adopted in the fabrication of high-quality TI films of Bi_2Se_3, Bi_2Te_3, and Sb_2Te_3 on substrates including sapphire,[12] $SrTiO_3$,[13] and also Si.[9] Such an exotic feature of TIs and simplicity of growth make Bi_2Te_3, Bi_2Se_3, and Sb_2Te_3 the ideal candidates for applications in ultrafast transistors, quantum electronics, quantum computing, spintronics, thermoelectric devices, low dissipation devices, etc. In addition to research efforts on the electronic and transport properties of TIs, much work has been carried out on their optical properties. Many theoretical studies have been focused on the response of the surface states to light, and several worthy progressive studies have been reported, including the Dirac surface state assisted high-performance broadband photodetection from infrared to terahertz,[14] the circularly polarized light induced helicity-dependent current,[15] the nonlinearity induced passive mode-locked lasers,[16] the warping effect enhanced relative signal-to-noise ratio (SNR),[17] and the linearly polarized light induced polarization dependent photocurrents.[18]

Zhang *et al.*[14] predicted that the TI Dirac-like surface state can have strong optical absorption. The surface absorption is determined by the fine-structure constant α, and it is uniform and independent of the wavelength. It is similar to another Dirac material, graphene. The absorbance is $\pi\alpha$ for graphene, and for 3D TIs, the absorbance is half of the result of graphene. The optical absorbance from the surface states of the Bi_2Te_3 film can increase by about 50% resulting from the warping effect.[17] In addition, the 3D TI's SNR is higher than that of $Hg_{1-x}Cd_xTe$, which has been widely used for infrared photon detection. The enhancement of the absorption and SNR make TIs comparable to graphene in photoconductive detectors. Photodetectors based on graphene

a)songyuxin@gmail.com
b)shumin@mail.sim.ac.cn

have already made substantial progress. In 2009, IBM demonstrated an ultrafast transistor based photodetector made from graphene.[19] A modulation speed of up to 40 GHz and a responsivity of up to 0.5 mAW^{-1} were demonstrated. Gan *et al*. demonstrated a waveguide-integrated graphene photodetector with a photon responsivity exceeding 0.1 AW^{-1} between 1450 and 1590 nm[20] while Liu *et al*. reported a graphene double-layer heterostructure with responsivity up to 1 AW^{-1} in the mid-infrared spectral range.[21] Research on TI photodetectors has just started recently. For a polycrystalline Bi_2Te_3 photodetector,[11] the photoresponsivity was reported in the order of 10^{-5} AW^{-1}. While for the one made of Sb_2Te_3 grown on sapphire, an impressive responsivity under 980 nm light illumination was estimated to be 21.7 AW^{-1}.[12] Although research on TIs has just begun, the high absorption and SNR may make TI detectors superior to graphene detectors. Furthermore, typical 3D TIs can be monolithically grown directly on Si at a CMOS compatible temperature, which promises future high density integration.

In this letter, Si-based Bi_2Te_3 photodetectors with responses to 1064 nm and 1550 nm light illumination at room temperature are demonstrated. This study shows that TI based photodetectors could be one of the candidate detectors for future Si photonics.

The Bi_2Te_3 thin film was grown on a semi-insulating Si substrate by MBE with a thickness of 50 nm. Atomic force microscopy (AFM) was used to study the surface morphology. The schematic of the Bi_2Te_3 photodetector structure and the corresponding measurement setup is illustrated in Figure 1. The HNO_3:CH_3COOH:H_2O_2:H_2O mixed solution was adopted to etch Bi_2Te_3 mesas with a preciously controlled etching rate and avoid the undercutting.[22] The mesa edges were examined using a scanning electron microscope. Due to the unstable Te-terminated surface, oxygen and water molecules in air can slightly oxidize the Bi_2Te_3 surface.[23] After etching, SiO_2 was deposited by inductively coupled plasma chemical vapor deposition at 80 °C to form a passivation layer. Then, the Ti/Au electrodes were achieved by electron beam evaporation on top of the Bi_2Te_3 film, which exhibits a linear dependence, suggesting that ideal Ohmic contacts were formed between the electrodes and the Bi_2Te_3 film from the I–V test in the dark.

A Hewlett Packard 4156 A precision semiconductor parameter analyzer was employed to evaluate the electronic transport characteristics of the Bi_2Te_3 photodetectors. Circular-polarized semiconductor lasers at the wavelengths of 1064 nm and 1550 nm were used to normally illuminate the device after being coupled into fibers. A Melles Griot universal optical power meter was used to measure the incident optical power. The incident power range for 1064 nm and 1550 nm was 0.67–2.8 mW and 0.194–0.389 mW, respectively. All the measurements were carried out at room temperature. The responsivity (R) and quantum efficiency (η) of this device were calculated according to the following equations, respectively:[12]

$$R = \frac{I_{ph}}{P_{opt}}, \tag{1}$$

$$\eta = R\left(\frac{hc}{q\lambda}\right), \tag{2}$$

where I_{ph}, P_{opt}, h, c, q and λ are the photocurrent, the light power of the effective illuminated area, the Planck's constant, the light velocity in vacuum, the electron charge, and the wavelength of incident light, respectively.

Figure 2 presents the AFM image of the Bi_2Te_3 film. The root mean square (RMS) roughness of the Bi_2Te_3 film is 1.29 nm. Surface steps with a height of 1 nm can be observed clearly, which correspond to the thickness of a quintuple layer with five Te-Bi-Te-Bi-Te atomic layers. The existence of clear surface steps indicates high crystal quality.

Photocurrent under different bias voltages and light powers was investigated, and the results after the removal of the background current are shown in Figure 3. Figures 3(a) and 3(c) present the photocurrent of a typical device under different incident powers at the wavelength of 1064 nm and 1550 nm, respectively. Obviously, the photocurrent exhibits a high dependence on the bias voltage and the incident light power. Along with the increasing bias voltage, an approximately

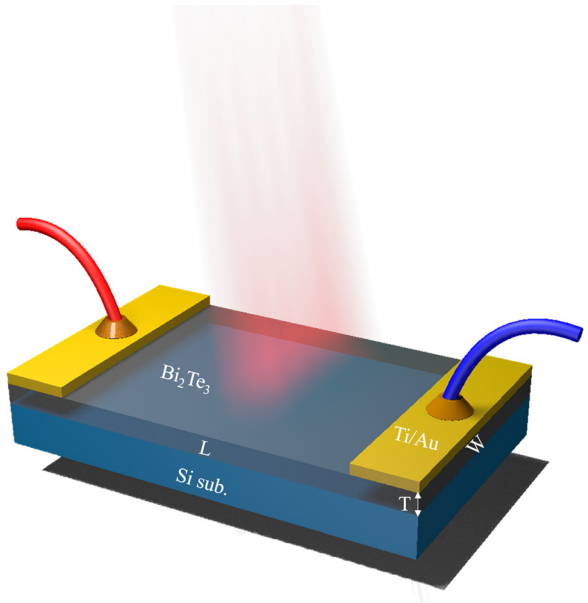

FIG. 1. The schematic of the TI Bi_2Te_3 photodetector and the measurement method. The dimensions of the Bi_2Te_3 for the device are length (L) = 1000 μm, width (W) = 500 μm, and thickness (T) = 50 nm.

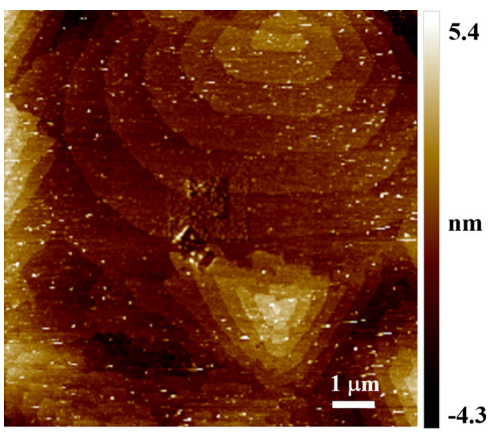

FIG. 2. AFM image of the Bi_2Te_3 film on Si.

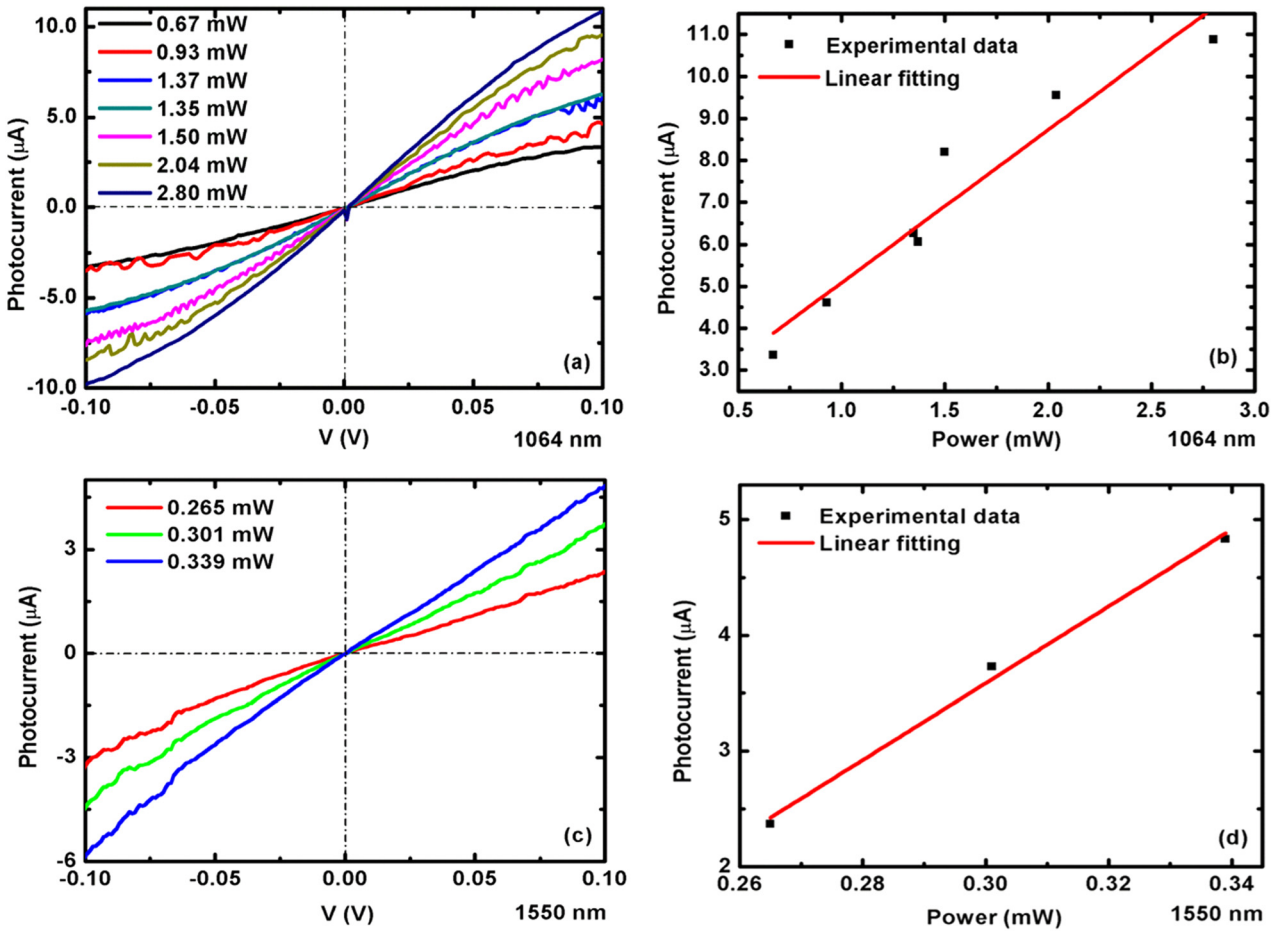

FIG. 3. Typical photocurrent-voltage curves of the Bi_2Te_3 photodetector at different incident powers under 1064 nm (a) and 1550 nm (c) illumination, respectively. (b) and (d) show the photocurrent under different excitation powers at 0.1 V corresponding to (a) and (c), respectively. The red line is a linear fit of the data points.

linear increasing tendency of photocurrent can be observed. Given the fact that the bias voltage facilitates the separation and transport of photon-excited carriers, collection of photo-generated carriers will increase significantly with the increase in the electric field. It is obvious that at the higher excitation intensity, more electron-hole pairs are generated, which is consistent with the observed fact that the photocurrent increases monotonously with the increase in the excitation power. In order to have a more intuitive observation of the photocurrent-excitation power relation, the photocurrent under different excitation powers at 0.1 V is plotted and linearly fitted in Figures 3(b) and 3(d) for 1064 nm and 1550 nm, respectively. Based on Eq. (1), Eq. (2), and the slope of the linear fitting curve, the responsivity for the device is 3.64×10^{-3} AW^{-1} for 1064 nm and 3.32×10^{-2} AW^{-1} for 1550 nm, respectively. The quantum efficiency is 0.424% for 1064 nm and 2.66% for 1550 nm.

The light path diagram of the Bi_2Te_3 photodetector on Si is schematically presented in Figure 4(a). The relationship of the incident light intensity-absorption coefficient for Bi_2Te_3 follows Eq. (3), where I, I_O, α, and d represent the light intensity, original incident light intensity, absorption coefficient, and thickness of the Bi_2Te_3 film, respectively. There are two interfaces of the device, Bi_2Te_3 and Si and Bi_2Te_3 and air. Reflections exist for both the interfaces. The interfacial reflection coefficients between air and Bi_2Te_3 are up to 53% for 1064 nm and 60% for 1550 nm, while those between Bi_2Te_3 and Si are 7.8% for 1064 nm and 14.7% for 1550 nm.[24] The absorption coefficients for different incident light wavelengths are also distinct, which are 7.0×10^5 cm^{-1} for 1064 nm and 4.2×10^5 cm^{-1} for 1550 nm, respectively. After multiple reflections, the relationship of the light intensity after absorption by the Bi_2Te_3 film and the original incident light intensity can be expressed by Eq. (4), where I_∞, R_C, and R_C' represent the light intensity after absorption by the Bi_2Te_3 film, reflection coefficient between air and the Bi_2Te_3 film, and reflection coefficient between the Bi_2Te_3 film and Si, respectively.

$$I = I_O e^{-ad}, \tag{3}$$

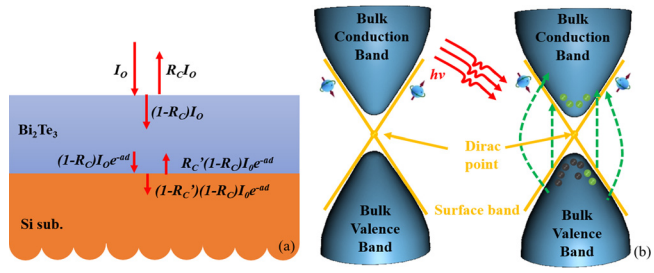

FIG. 4. Schematic diagram of the light path of the Bi_2Te_3 photodetector on Si (a) and the energy band of the Bi_2Te_3 (b).

$$I_\infty = \frac{R_C + (1-R_C)(1-R'_C)e^{-ad}}{1-(1-R_C)R'_C e^{-2ad}} I_O. \quad (4)$$

Obviously, the reflection of most of the incident light has been caused by the large reflection rate. Considering this non-negligible loss, the quantum efficiency can be revised by dividing 0.457 for 1064 nm and 0.358 for 1550 nm (the other portion is reflected by the interfaces and transmitted into Si). After revision, the internal quantum efficiency of the device is 0.9% under the wavelength of 1064 nm, and it corresponds to 7.4% for the case of 1550 nm. Under the same incident power, the longer wavelength leads to a larger number of photons, thereby a higher photocurrent and larger responsivity are expected. The performance of the present device in terms of responsivity and quantum efficiency is much better than those of the published polycrystalline Bi_2Te_3[11] based devices. The responsivity is 2–3 orders higher.

To explain further about the photon response in our photodetector device, an energy-dispersion diagram is used to elucidate the excitation processes shown in Figure 4(b). As a TI, Bi_2Te_3 has both bulk states and surface states. Many possible interband optical transition channels among these states exist.[25] For Bi_2Te_3, the bandgap measured by angle-resolved photoemission spectroscopy is 0.165 eV[7] while that for Si is 1.12 eV. The photocurrent would mainly consist of four parts: the photoconductivity effect of the Bi_2Te_3 bulk and the surface states, transitions between the surface states and the bulk states, and the contribution of Si. For illumination at 1064 nm, Si shows little absorption to the incident light since most light is absorbed by Bi_2Te_3 before reaching Si. While for 1550 nm, Si is transparent to the incident photons, so that all the photon generated current is from Bi_2Te_3. Both photons of 1064 nm and 1550 nm light have enough energy to excite electrons from the valence band to the conduction band of Bi_2Te_3. Photon absorption and carrier excitation are mainly attributed to the bulk state of Bi_2Te_3 because of the much less surface density of the TI Bi_2Te_3. Transitions between the surface states and the bulk states from the valence band to the conduction band are also allowed.[25] If the illumination energy is below the band gap of Bi_2Te_3, electron–hole pairs can still be generated through surface band excitations. In that circumstance, the photocurrent would be mostly generated from the TI's surface states. Based on the present results, it is evident that the photocurrent is mainly from Bi_2Te_3 other than Si. Since both excitation lights have a larger photon energy than the bandgap of Bi_2Te_3, the contribution of band-to-band transition between the conduction and the valence band must exist. Further investigation is required to ascertain contributions from other possible transition channels and their percentages.

In summary, we reported a monocrystalline Bi_2Te_3 photoconductive detector on Si grown by MBE, which is compatible with CMOS technology and can be monolithically integrated on Si. The as-fabricated TI photodetector exhibits a high response to photons at 1064 nm and 1550 nm at room temperature. The responsivity and the quantum efficiency are much better than polycrystalline Bi_2Te_3 based devices. The responsivity and the internal quantum efficiency of the device are 3.64×10^{-3} AW^{-1} and 0.9% for 1064 nm and 3.32×10^{-2} AW^{-1} and 7.4% for 1550 nm, respectively. This study suggests that the TI (Bi_2Te_3) photodetectors have potential applications in future Si photonics.

The authors would like to acknowledge the financial support from the Natural Science Foundation of China (Grant No. 61404153), the Shanghai Pujiang Program (Grant No. 14PJ1410600), the Key Program of Natural Science Foundation of China (Grant No. 61334004), the National Basic Research Program of China (973) (Grant No. 2014CB643902), the Strategic Priority Research Program of the Chinese Academy of Sciences (Grant No. XDA5-1), the Key Research Program of the Chinese Academy of Sciences (Grant No. KGZD-EW-804), the Creative Research Group Project of Natural Science Foundation of China (Grant No. 61321492), the International Collaboration and Innovation Program on High Mobility Materials Engineering of Chinese Academy of Sciences, and the Open Program of State Key Laboratory of Functional Materials for Informatics.

[1]M. M. Waldrop, Nat. News **530**, 144 (2016).
[2]D. Liang and J. E. Bowers, Nat. Photonics **4**, 511 (2010).
[3]R. Soref, IEEE J. Sel. Top. Quantum Electron. **12**, 1678 (2006).
[4]L. Vivien, J. Osmond, D. Marris-Morini, P. Crozat, E. Cassan, J. M. Fédéli, S. Brision, J. F. Damlencourt, V. Mazzochi, D. Van Thourhout, and J. Brouckaert, in *IEEE International Conference on Group IV Photonics GFP* (2009), Vol. 1, p. 10.
[5]L. Chen, P. Dong, and M. Lipson, Opt. Express **16**, 11513 (2008).
[6]S. Feng, Y. Geng, K. M. Lau, and A. W. Poon, *IEEE International Conference on Group IV Photonics GFP* (2012), Vol. 37, p. 51.
[7]Y. L. Chen, J. G. Analytis, J. H. Chu, Z. K. Liu, S. K. Mo, X. L. Qi, H. J. Zhang, D. H. Lu, X. Dai, Z. Fang, S. C. Zhang, I. R. Fisher, Z. Hussain, and Z. X. Shen, Science **325**, 178 (2009).
[8]H. Zhang, C. Liu, X. Qi, X. Dai, Z. Fang, and S. Zhang, Nat. Phys. **5**, 438 (2009).
[9]Y. Y. Li, G. Wang, X. G. Zhu, M. H. Liu, C. Ye, X. Chen, Y. Y. Wang, K. He, L. L. Wang, X. C. Ma, H. J. Zhang, X. Dai, Z. Fang, X. C. Xie, Y. Liu, X. L. Qi, J. F. Jia, S. C. Zhang, and Q. K. Xue, Adv. Mater. **22**, 4002 (2010).
[10]H. Cao, R. Venkatasubramanian, C. Liu, J. Pierce, H. Yang, M. Z. Hasan, Y. Wu, and Y. P. Chen, Appl. Phys. Lett. **101**, 162104 (2012).
[11]H. Zhang, J. Yao, J. Shao, H. Lu, S. Li, D. Bao, C. Wang, and G. Yang, Sci. Rep. **4**, 5876 (2014).
[12]K. Zheng, L. B. Luo, T. F. Zhang, Y. H. Liu, Y. Q. Yu, R. Lu, H. L. Qiu, Z. J. Li, and J. C. Andrew Huang, J. Mater. Chem. C **3**, 9154 (2015).
[13]P. H. Le, K. H. Wu, C. W. Luo, and J. Leu, Thin Solid Films **534**, 659 (2013).
[14]X. Zhang, J. Wang, and S. C. Zhang, Phys. Rev. B **82**, 245107 (2010).
[15]P. Hosur, Phys. Rev. B **83**, 035309 (2011).
[16]J. Koo, J. Lee, C. Chi, and J. H. Lee, J. Opt. Soc. Am. B **31**, 2157 (2014).
[17]J. M. Shao, H. Li, and G. W. Yang, Nanoscale **6**, 3513 (2014).
[18]J. D. Yao, J. M. Shao, S. W. Li, D. H. Bao, and G. W. Yang, Sci. Rep. **5**, 14184 (2015).
[19]F. Xia, T. Mueller, Y. Lin, A. Valdes-Garcia, and P. Avouris, Nat. Nanotechnol. **4**, 839 (2009).
[20]X. Gan, R. J. Shiue, Y. Gao, I. Meric, T. F. Heinz, K. Shepard, J. Hone, S. Assefa, and D. Englund, Nat. Photonics **7**, 883 (2013).
[21]C. H. Liu, Y. C. Chang, T. B. Norris, and Z. Zhong, Nat. Nanotechnol. **9**, 273 (2014).
[22]T. Ngai and U. Ghoshal, 27thInternational Conference on Thermoelectrics (2007).
[23]H. Liu and P. D. Ye, Appl. Phys. Lett. **99**, 052108 (2011).
[24]R. Clasen, P. Grosse, A. Krost, and F. Levy, *Non-Tetrahedrally Bonded Elements and Binary Compounds I* (Springer, New York, 1998).
[25]L. L. Li, W. Xu, and F. M. Peeters, J. Appl. Phys. **117**, 175305 (2015).